World Journal of Research and Review (WJRR)
ISSN:2455-3956, Volume-3, Issue-5, November 2016 Pages 01-09

A Simulation Study of the Effect of Powerful High-Frequency Radio Waves on the Behavior of Super-Small-Scale Irregularities in the F-layer Ionospheric Plasma

O.V. Mingalev, M.N. Melnik, V.S. Mingalev

Abstract **- Magnetic field aligned super-small-scale irregularities in the concentration of charged particles are often observed in the Earth's ionosphere and magnetosphere. Earlier, the time evolution of such irregularities was studied with the help of the mathematical model, developed in the Polar Geophysical Institute. This model is based on a numerical solution of the Vlasov-Poisson system of equations. This mathematical model is used in the present paper. The purpose of the present paper is to examine numerically how high-power high-frequency radio waves, utilized for artificial heating experiments and pumped into the ionosphere by ground-based ionospheric heaters, influence on the time evolution of the super-small-scale irregularities present naturally in the F-layer ionospheric plasma. The results of simulation indicate that a presence of high-power high-frequency radio wave ought to influence essentially on the behavior of physically significant parameters of the plasma inside and in the vicinity of the irregularity.**

Index Terms **- ionospheric plasma, super-small-scale irregularities, numerical simulation.**

I. INTRODUCTION

In the Earth's ionosphere, electron density irregularities are present always. Spatial sizes of these irregularities can vary from thousands of kilometers to a few centimeters. The electron density depletions and increases inside irregularities can lie in the range from a few portions to some tens of percentages. Various types of irregularities can exist in the ionosphere, in particular, large-scale irregularities in the ionospheric F layer [1]-[6], middle-scale irregularities [7]-[8], short-scale irregularities [9]-[14], and super-small-scale irregularities [15]. It is known that not large-scale irregularities are predominately magnetic field aligned.

The electron density irregularities in the ionosphere can be formed not only by natural physical processes but also as a result of active experiments. In particular, ionospheric irregularities may be formed by high-power high-frequency radio waves, pumped into the ionosphere by ground based ionospheric heaters [15]-[19]. These waves can cause a variety of physical processes in the ionospheric plasma. These processes can result in the formation of not only large-scale irregularities in the electron temperature and electron concentration but also super-small-scale irregularities in the concentration of charged particles.

For investigation of the behavior of the artificially created irregularities in the ionospheric plasma not only the experimental and theoretical but also computational studies may be applied. The formation of large-scale irregularities by powerful high frequency waves, utilized for artificial heating experiments and pumped into the ionosphere by ground-based ionospheric heaters, was investigated with the help of mathematical models in some studies (for example, see [16-29]). The formation of the super-small-scale irregularities in the concentration of charged particles in the F-layer ionosphere by powerful high frequency waves was considered and simulated in the study by Eliasson and Stenflo [30]. It should be emphasized that such irregularities may be formed in the ionospheric plasma not only artificially but also by natural processes [15].

The time evolution of super-small-scale irregularities was investigated with the help of the mathematical model, developed in the Polar Geophysical Institute, under natural conditions without action of powerful high frequency waves in studies [31]-[33]. It may be expected that powerful high frequency waves can influence on the behavior of existent super-small-scale irregularities.

In the present study, the mathematical model, developed earlier in the Polar Geophysical Institute, is utilized for numerical investigation of the effect of high-power high-frequency radio waves on the time evolution of the super-small-scale irregularities, created naturally in the F-layer ionospheric plasma. The present work is the continuation of the investigation begun in the study of Mingalev et al. [33], with new simulation results being submitted in the present paper.

II. MATHEMATICAL MODEL

To examine numerically how high-power high-frequency radio waves, pumped into the ionosphere by ground-based ionospheric heaters, influence on the time evolution of the super-small-scale irregularities, present naturally in the F-layer ionospheric plasma, the mathematical model, developed earlier in the Polar Geophysical Institute [33], is utilized. This model is based on a numerical solution of the Vlasov-Poisson system of equations.

At F-layer altitudes, the ionospheric plasma is supposed to be a rarefied compound consisting of electrons and positive ions in the presence of a strong, external, uniform magnetic field. The studied irregularities are

O.V. Mingalev, Polar Geophysical Institute, Russian Academy of Sciences, Apatity, Murmansk Region, Russia.
M.N. Melnik, Polar Geophysical Institute, Russian Academy of Sciences, Apatity, Murmansk Region, Russia.
V.S. Mingalev, Polar Geophysical Institute, Russian Academy of Sciences, Apatity, Murmansk Region, Russia.

This work was partly supported by the Division of the Physical Sciences of the Russian Academy of Sciences through the program "Dynamics of rarefied plasma in space and laboratory".

geomagnetic field-aligned, with their cross-sections being circular. The initial cross-section diameters of the irregularities are supposed to be several Debye lengths (no more than about 100) [15].

At F-layer levels, the mean free path of particles (electrons and ions) between successive collisions is much more than the cross-section diameters of the considered irregularities. Therefore, the plasma is assumed to be collisionless. Kinetic processes in such plasma are described by the Vlasov-Poisson system of equations which has been considered, for example, in the studies by Hockney and Eastwood [34], and Birdsall and Langdon [35]. This system may be written as follows:

$$\frac{\partial f_a}{\partial t}+\left(\mathbf{v},\frac{\partial f_a}{\partial \mathbf{x}}\right)+\frac{q_a}{m_a}\left(\mathbf{E}+\left[\mathbf{v}\times\mathbf{B}_0\right],\frac{\partial f_a}{\partial \mathbf{v}}\right)=0,\ a=i,e, \tag{1}$$

$$\Delta\varphi(\mathbf{x},t)=-\frac{1}{\varepsilon_0}\rho(\mathbf{x},t), \tag{2}$$

$$\mathbf{E}(\mathbf{x},t)=-\nabla\varphi(\mathbf{x},t),$$

$$\rho(\mathbf{x},t)=e_0(n_i-n_e),\quad n_a(\mathbf{x},t)=\int f_a(t,\mathbf{x},\mathbf{v})d\mathbf{v},$$

where $f_a(t,\mathbf{x},\mathbf{v})$, $n_a(\mathbf{x},t)$, m_a, and q_a are, respectively, the distribution function, concentration, mass, and charge of particles of type a, $\mathbf{x}$ is the space coordinate vector, $\mathbf{v}$ is the velocity, $\mathbf{B}_0$ is the external magnetic field, $\mathbf{E}$ is the self-consistent electric field, $\varphi(\mathbf{x},t)$ is the electric field potential, $\rho(\mathbf{x},t)$ is the electric charge density, ε_0 is the dielectric constant of free space, and e_0 is the proton charge. The Vlasov kinetic equation (1) describes the evolution of the distribution functions of charged particles and the Poisson equation (2) describes the self-consistent electric field.

It may be recalled that the investigated irregularities are geomagnetic field-aligned. Their longitudinal sizes are much more than the cross-section diameters. Gradients of the plasma parameters in the longitudinal direction are much less than those in a plane perpendicular to a magnetic field in the vicinity of the irregularity. Therefore, plasma parameters in the vicinity of the irregularity may be considered as independent on the longitudinal coordinate. This simplification allow us to consider a two dimensional flow of plasma in a plane perpendicular to a magnetic field line. Therefore, the mathematical model, developed earlier in the Polar Geophysical Institute and utilized in [31]-[33], is two-dimensional. This mathematical model is used in the present study, too.

A macroparticle method is utilized for numerical solving of the Vlasov equations (1). A finite-difference method is used for numerical solving of the Poisson equation (2). In the applied version of the mathematical model a motion of the positive ions is taken into account. In the model calculations, a two-dimensional simulation region, lain in the plane perpendicular to the magnetic field line, is a square and its side length is equal to 128 Debye lengths of the plasma. The quantity of the grid cells is 1024×1024 and the average number of macro-particles in the Debye cell for the model plasma is 2^{15}. Detailed description of the utilized mathematical model may be found in the study of Mingalev et al. [33].

III. PRESENTATION AND DISCUSSION OF RESULTS

Calculations with the help of the utilized two-dimensional mathematical model can be made for various conditions in the ionospheric plasma. The results of calculations to be presented in this paper were obtained using the input parameters of the model typical for the nocturnal F-layer ionospheric plasma at the level of 300 km. At this level, the plasma, apart from electrons, contains positive ions, with the oxygen ion, O^+, being the bulk of ion content (99%). The value of the non-disturbed electron concentration (equal to the positive ion concentration), n_0, is 10^{11} m^{-3}. The electron and ion temperatures are supposed to be equal to 1213 K and 930 K, respectively. At the initial moment, the bulk flow velocities of electrons and positive ions, $\boldsymbol{u_e}$ and $\boldsymbol{u_i}$ respectively, are assumed to be zero. The value of the magnetic field, B_0, is $4.4\cdot10^{-5}$ T.

Under chosen conditions in the ionospheric plasma, the equilibrium plasma frequency, ω^0_{pe}, is $1.78\cdot10^7$ s^{-1}, the frequency of cyclotron oscillations of electrons, ω_{ce}, is $7.74\cdot10^6$ s^{-1}, the Debye length of the plasma, λ^0_{De}, is equal to $7.6\cdot10^{-3}$ m, the equilibrium period of Langmuir oscillations of electrons, T_{pe}, is $3.52\cdot10^{-7}$ s, the equilibrium period of Langmuir oscillations of oxygen ions, T_{pi}, is approximately a factor of 171 larger than the equilibrium period of Langmuir oscillations of electrons ($T_{pi} \approx 171\cdot T_{pe}$), the period of cyclotron oscillations of electrons, T_{ce}, is approximately a factor of 2.3 larger than the equilibrium period of Langmuir oscillations of electrons ($T_{ce} \approx 2.3\cdot T_{pe}$), and the mean free time of electron between successive collisions with other particles is larger than the equilibrium period of Langmuir oscillations of electrons by a factor of about 1047.

The simulation results to be presented in this paper were obtained for the following initial state of the irregularity inside the two-dimensional simulation region. The spatial distribution of the electron concentration (equal to the positive ion concentration at the initial moment), contains a circular irregularity at the center of the simulation region. Beyond this irregularity, the electron concentration is homogeneous and coincides with the non-disturbed electron concentration, n_0. The initially created irregularity has the cross-section diameter of $12\lambda^0_{De}$. Inside the irregularity, homogeneity of the plasma is broken and a part of charged particles travels from the internal circle, having the diameter of $6\lambda^0_{De}$, into the external ring, surrounding the internal circle. The relative decrease of the concentration of charged particles, $(n_0 - n_e)/n_0$, is equal to 0.1 in the internal circle at the initial moment, that is, 10 percent of charged particles were displaced from the center of the irregularity to its periphery, with the plasma having been electrically neutral at the initial moment.

We have calculated the time evolution of the distribution functions of charged particles as well as self-consisting electric field for two distinct on principle situations. The first situation corresponds to absence of external electric field, whereas the second situation corresponds to presence of external electric field which

represents a high-power high-frequency radio wave, pumped into the ionosphere by a ground-based ionospheric heater. It is supposed that this radio wave illuminates the two-dimensional simulation region.

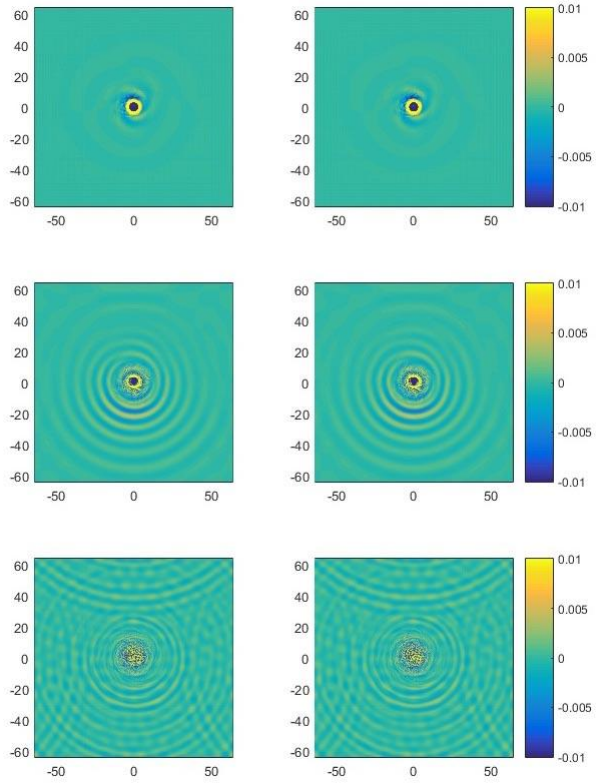

Fig 1: The calculated spatial distributions of the normalized electric charge density, $(n_i - n_e) / n_0$, in the plane perpendicular to the magnetic field. The vector of the magnetic field lies on the axis, perpendicular to the simulation region, and is directed downwards. The normalized distances, $\boldsymbol{X} / \lambda^0_{De}$ and $\boldsymbol{Y} / \lambda^0_{De}$, that is, the distances in units of the Debye length, λ^0_{De}, from the central point of the simulation region are shown on the horizontal ($\boldsymbol{X}$) and vertical ($\boldsymbol{Y}$) axes. For the first situation, correspondent to absence of an external electric field, the results are presented in the left column, whereas, for the second situation, correspondent to presence of the high-power high-frequency radio wave, the results are shown in the right column. The results are given for the following moments: $t = 5.2 \cdot T_{pe}$ (top panel), $t = 25 \cdot T_{pe}$ (middle panel), $t = 100 \cdot T_{pe}$ (bottom panel).

In the second situation, the high-frequency radio wave, radiated by a ground-based ionospheric heater, is supposed to propagate along a magnetic field line up to the reflection point, to turn back, and to propagate towards the Earth's surface along a magnetic field line, with the disturbing high-frequency radio wave becoming a standing wave. It may be noted that the described situation can be more probably realized at high latitudes where the direction of magnetic field is close to vertical.

As was noted earlier, the two-dimensional simulation region lies in the plane perpendicular to the magnetic field line. Therefore, the vector of the high-frequency wave's electric field, **E**, lies in the plane of the simulation region and has not a projection perpendicular to the simulation region. It is assumed that the disturbing high-frequency radio wave is ordinary and that its frequency, ω_0, is equal to the frequency of the electron hybrid resonance, namely, $\omega_0 = [(\omega^0_{pe})^2 + (\omega_{ce})^2]^{1/2}$. It turns out that the frequency of the disturbing high-frequency radio wave is approximately a factor of 1.09 larger than the equilibrium plasma frequency ($\omega_0 \approx 1.09 \cdot \omega^0_{pe}$). After the initial moment, the module of the vector of the high-frequency wave's electric field increases smoothly and, during the time interval of five periods of Langmuir oscillations of electrons, reaches the value of 0.49 V/m which is quite attainable, for example, for the heating facility near Tromso, Scandinavia. The vector of the high-frequency wave's electric field, **E**, rotates with the frequency equal to ω_0 in each point of the two-dimensional simulation region.

Simulation results, obtained for the first situation, correspondent to absence of an external electric field, indicate that, after initial moment, the spatial distribution of the electron concentration changes essentially while the positive ion concentration is retained practically invariable. It turns out that the initially created irregularity vanishes completely during a short period, with the plasma becoming electrically neutral in all simulation region at the moment near to the equilibrium period of Langmuir oscillations of electrons $\left(t \approx T_{pe}\right)$. Further calculations indicate that the changes in the electron concentration are continued and, after a short period, the irregularity arises again to a moment of about $(2.2 - 2.3)\, T_{pe}$, with the recovered irregularity almost completely coinciding with the initial one. Later, the cycle of vanishing and recovering of the irregularity is repeated again and again. Thus, the time evolution of the initially created irregularity is accompanied by periodic vibrations. The period of these vibrations is approximately a factor of 2.3 larger than the equilibrium period of Langmuir oscillations of electrons, with the former period coinciding with the period of cyclotron oscillations of electrons, T_{ce}. In the course of time, the amplitudes of the vibrations of the electron concentration decrease smoothly, with the irregularity decaying little by little.

In the process of evolution, additional almost symmetrical alternate rings with an excess of charge of different sign begin to appear around the initial irregularity situated in the center of the simulation region. In the course of time, these additional rings begin to fill up all simulation region, with the irregularity center remaining immovable.

It is of interest to note that, in the process of evolution, essential electric fields can arise at the points of the simulation region situated between the rings with an excess of charge of different sign, in particular, close to the center of the simulation region where the initially created irregularity has been situated.

Simulation results, obtained for the second situation, correspondent to presence of the high-power high-frequency radio wave, have both distinctions and common features with the results, obtained for the first situation correspondent to absence of external electric field.

The spatial distributions of the normalized electric charge density, calculated for some moments, are presented in Figure 1. It is seen that the results, obtained for two considered situations, have some common features. The

irregularities vanish and recover periodically, with its parameters fluctuating.

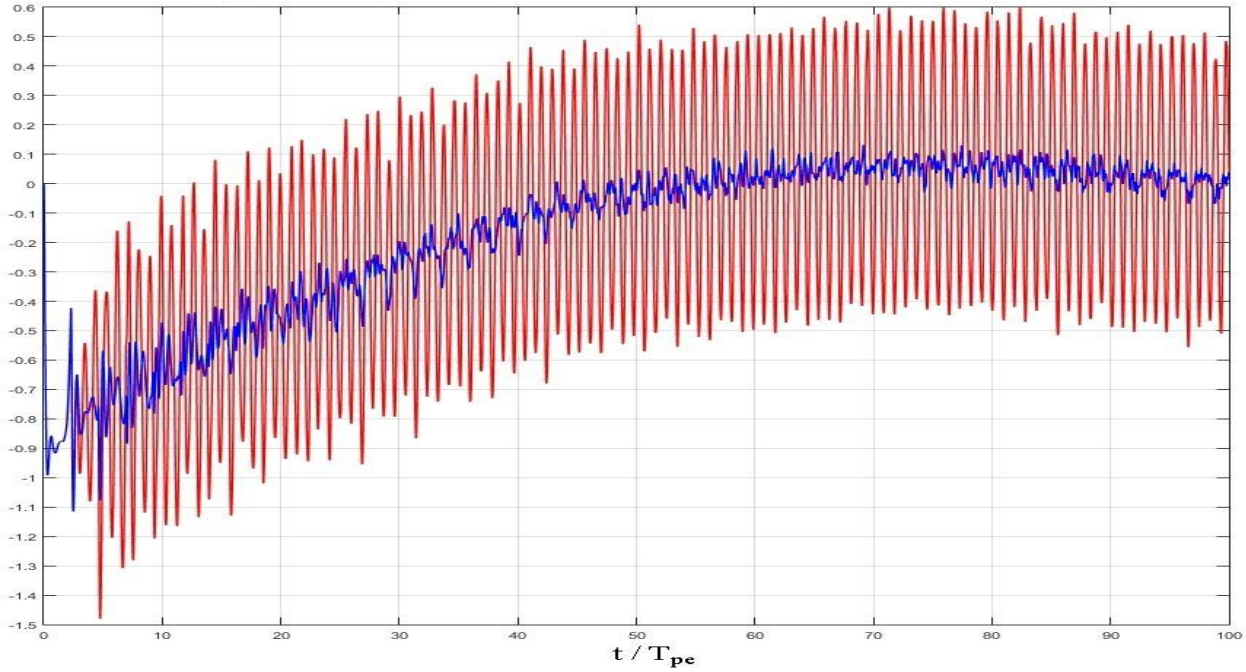

Fig 2: The time variations of one component of the electric field, namely E_x , lying in the plane perpendicular to the magnetic field, calculated at the point, displaced from the center of the simulation region in the ***X*** direction for a distance of three Debye lengths $\left(3\cdot\lambda_{De}^{0}\right)$. For the first situation, correspondent to absence of an external electric field, the results are shown by blue line, whereas, for the second situation, correspondent to presence of the high-power high-frequency radio wave, the results are shown by red line. The electric field component is given in V/m. The normalized time, t/T_{pe} , that is, the time in units of the equilibrium period of Langmuir oscillations of electrons, T_{pe} , is shown on the abscissa.

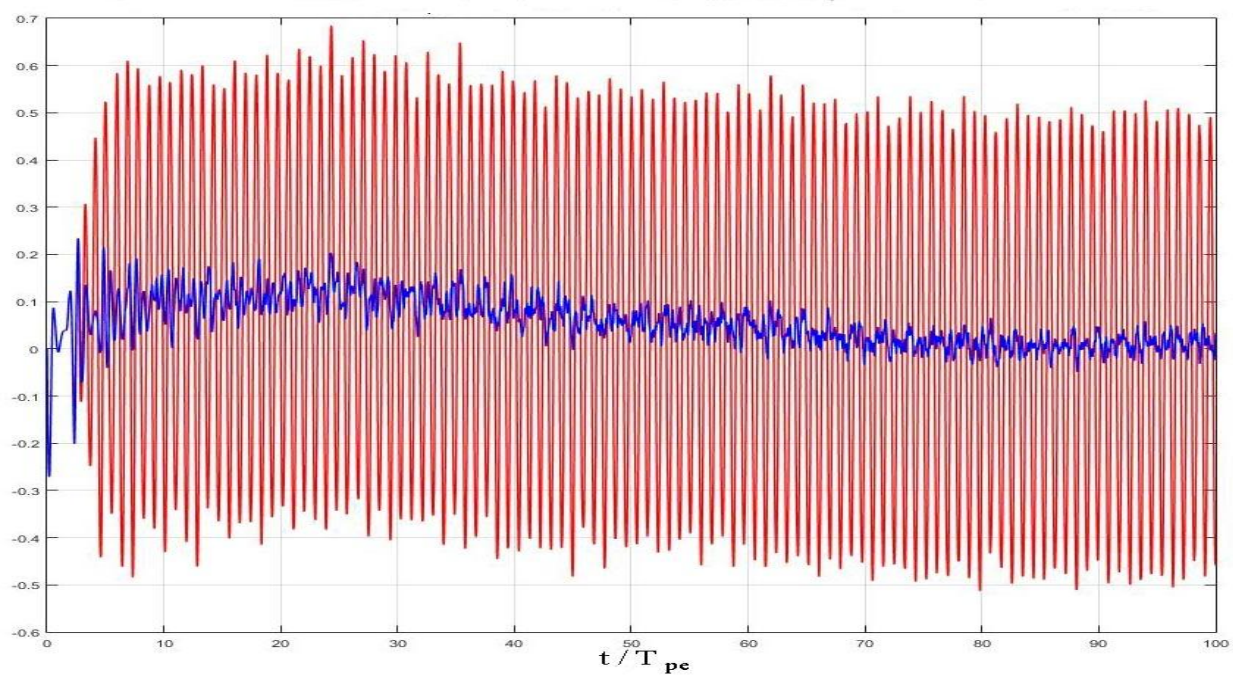

Fig 3: The time variations of one component of the electric field, namely E_y , lying in the plane perpendicular to the magnetic field, calculated at the point, displaced from the center of the simulation region in the ***X*** direction for a distance of three Debye lengths $\left(3\cdot\lambda_{De}^{0}\right)$. For the first situation, correspondent to absence of an external electric field, the results are shown by blue line, whereas, for the second situation, correspondent to presence of the high-power high-frequency radio wave, the results are shown by red line. The electric field component is given in V/m. The normalized

time, t/T_{pe}, that is, the time in units of the equilibrium period of Langmuir oscillations of electrons, T_{pe}, is shown on the abscissa.

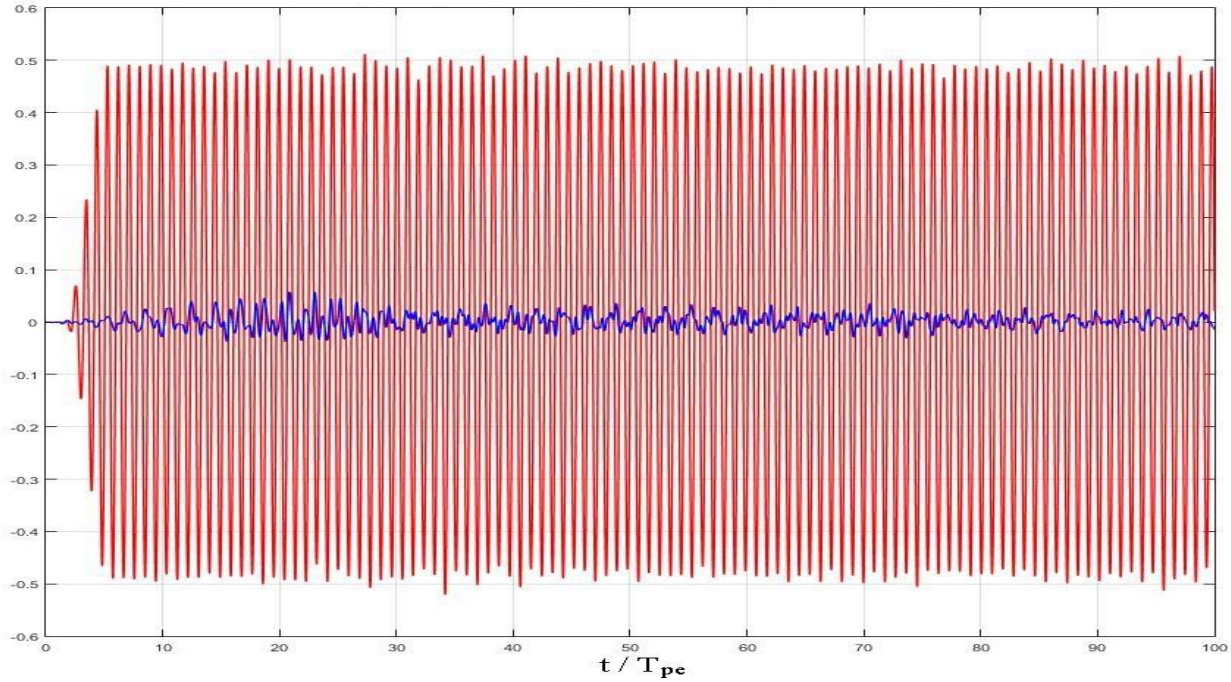

Fig 4: The time variations of one component of the electric field, namely E_x, lying in the plane perpendicular to the magnetic field, calculated at the point, displaced from the center of the simulation region in the ***X*** direction for a distance of sixteen Debye lengths $\left(16\cdot\lambda_{De}^{0}\right)$. For the first situation, correspondent to absence of an external electric field, the results are shown by blue line, whereas, for the second situation, correspondent to presence of the high-power high-frequency radio wave, the results are shown by red line. The electric field component is given in V/m. The normalized time, t/T_{pe}, that is, the time in units of the equilibrium period of Langmuir oscillations of electrons, T_{pe}, is shown on the abscissa.

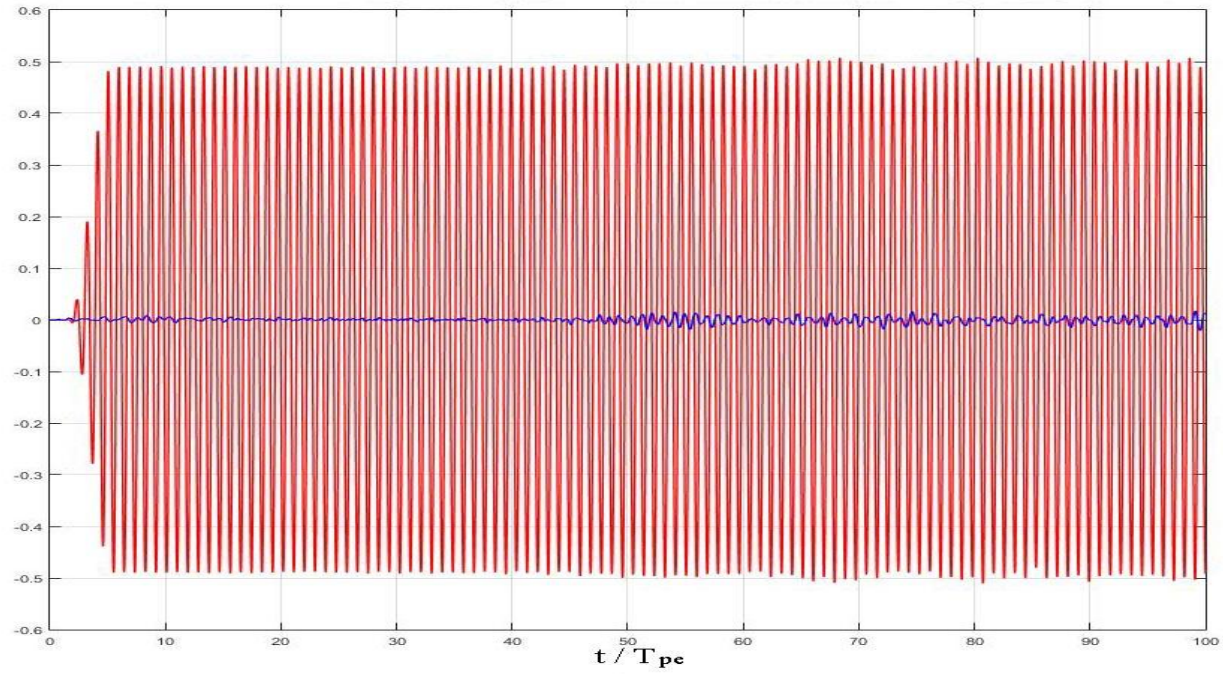

Fig 5: The time variations of one component of the electric field, namely E_y, lying in the plane perpendicular to the magnetic field, calculated at the point, displaced from the center of the simulation region in the ***X*** direction for a distance of sixteen Debye lengths $\left(16\cdot\lambda_{De}^{0}\right)$. For the first situation, correspondent to absence of an external electric field, the results are shown by blue line, whereas, for the second situation, correspondent to presence of the high-power high-frequency radio wave, the results are shown by red line. The electric field component is given in V/m. The normalized

time, t/T_{pe}, that is, the time in units of the equilibrium period of Langmuir oscillations of electrons, T_{pe}, is shown on the abscissa.

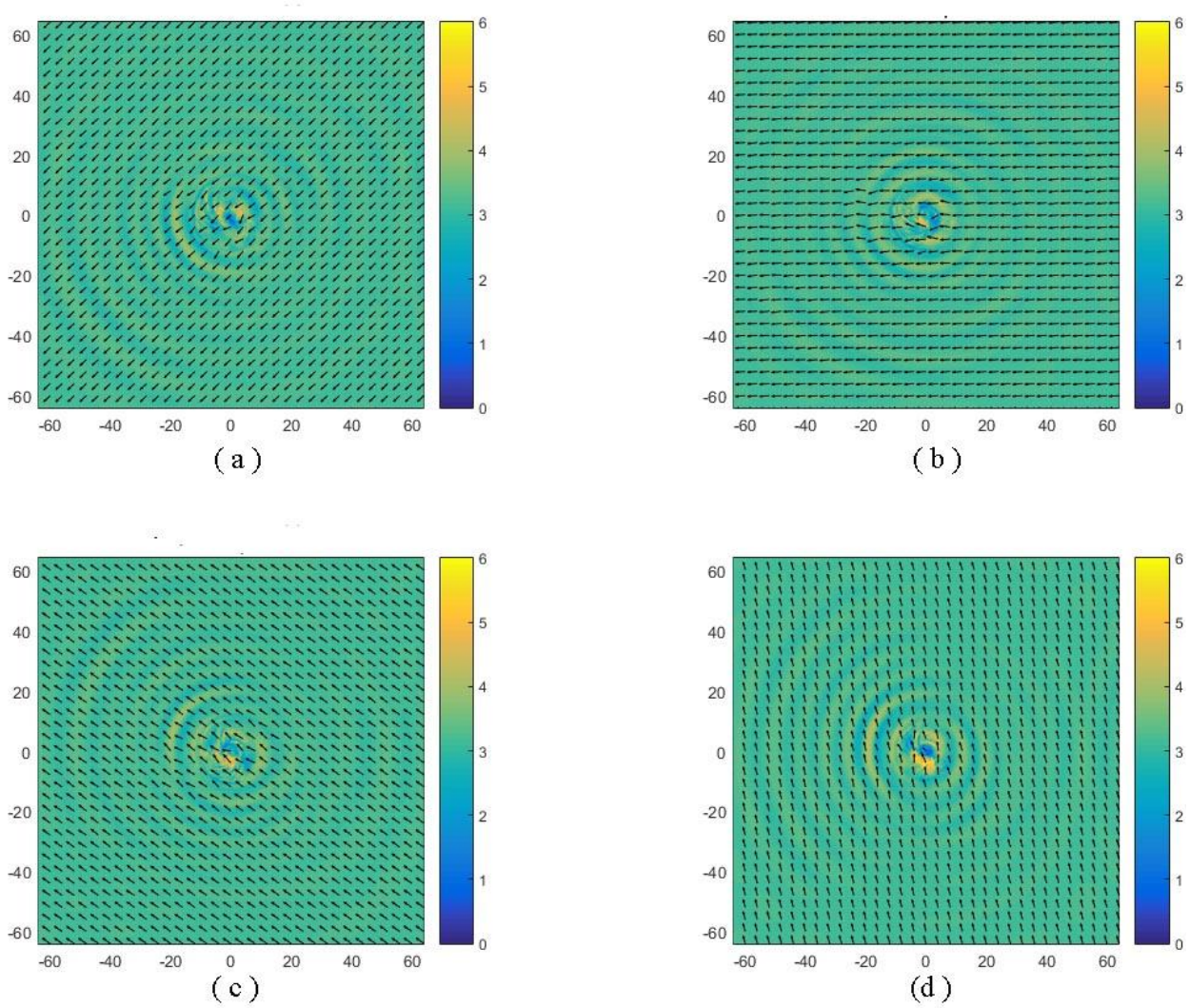

Fig 6: The spatial distributions of the vector of the bulk flow velocity of electrons, $\boldsymbol{u_e}$, calculated for the second situation, correspondent to presence of the high-power high-frequency radio wave, in the plane perpendicular to the magnetic field. The normalized distances, $\boldsymbol{X}/\lambda_{De}^{0}$ and $\boldsymbol{Y}/\lambda_{De}^{0}$, that is, the distances in units of the Debye length, λ_{De}^{0}, from the central point of the simulation region are shown on the horizontal ($\boldsymbol{X}$) and vertical ($\boldsymbol{Y}$) axes. The vector of the magnetic field lies on the axis, perpendicular to the simulation region, and is directed downwards. The colouration of the figures indicates the module of the velocity in km/s. The results are given for the following moments: (a) $t = 98.6 \cdot T_{pe}$, (b) $t = 99 \cdot T_{pe}$, (c) $t = 99.4 \cdot T_{pe}$, (d) $t = 99.8 \cdot T_{pe}$.

Examples of fluctuating parameters of the plasma are presented in Figures 2-5 where time variations of the electric field components at two points of the simulation region are shown. It is seen that the amplitudes of the electric field fluctuations, obtained for the second situation, correspondent to presence of the high-power high-frequency radio wave, are much more than those, obtained for the first situation, correspondent to absence of external electric field. The former amplitudes are close to the module of the vector of the external high-frequency wave's electric field (0.49 V/m).

Other distinction between the results, obtained for two considered situations, concerns the periods of the fluctuations. For the first situation, correspondent to absence of an external electric field, it is easy to see from Figures 2-5 that the electric field fluctuations posses of two main periods, namely, the period of Langmuir oscillation of electrons and period of cyclotron oscillations of electrons. In particular, the period of the fluctuations, having maximal amplitudes, is close to the period of cyclotron oscillations of electrons, which is approximately a factor of 2.3 larger than the period of Langmuir oscillations of electrons. Unlike, for the second situation, correspondent to presence of the high-power high-frequency radio wave, the period of the electric field fluctuations is close to the period of the vibrations of the disturbing high-frequency radio wave. The later period is approximately a factor of 0.92 smaller than the equilibrium period of Langmuir oscillations of electrons.

It is known that the ionospheric plasma at F-layer altitudes is strongly magnetized. As a consequence, the bulk flow velocities of electrons and positive ions, $\boldsymbol{u_e}$ and $\boldsymbol{u_i}$ respectively, in the direction perpendicular to the magnetic field **B** is strongly affected by the electric field **E,** with the

plasma transport perpendicular to the magnetic field lines following **E×B** direction. As was noted earlier, the vector of the high-power high-frequency wave's electric field, **E**, rotates in each point of the two-dimensional simulation region. Therefore, the bulk flow velocities of electrons and positive ions, $\boldsymbol{u_e}$ and $\boldsymbol{u_i}$ respectively, ought to rotate, too.

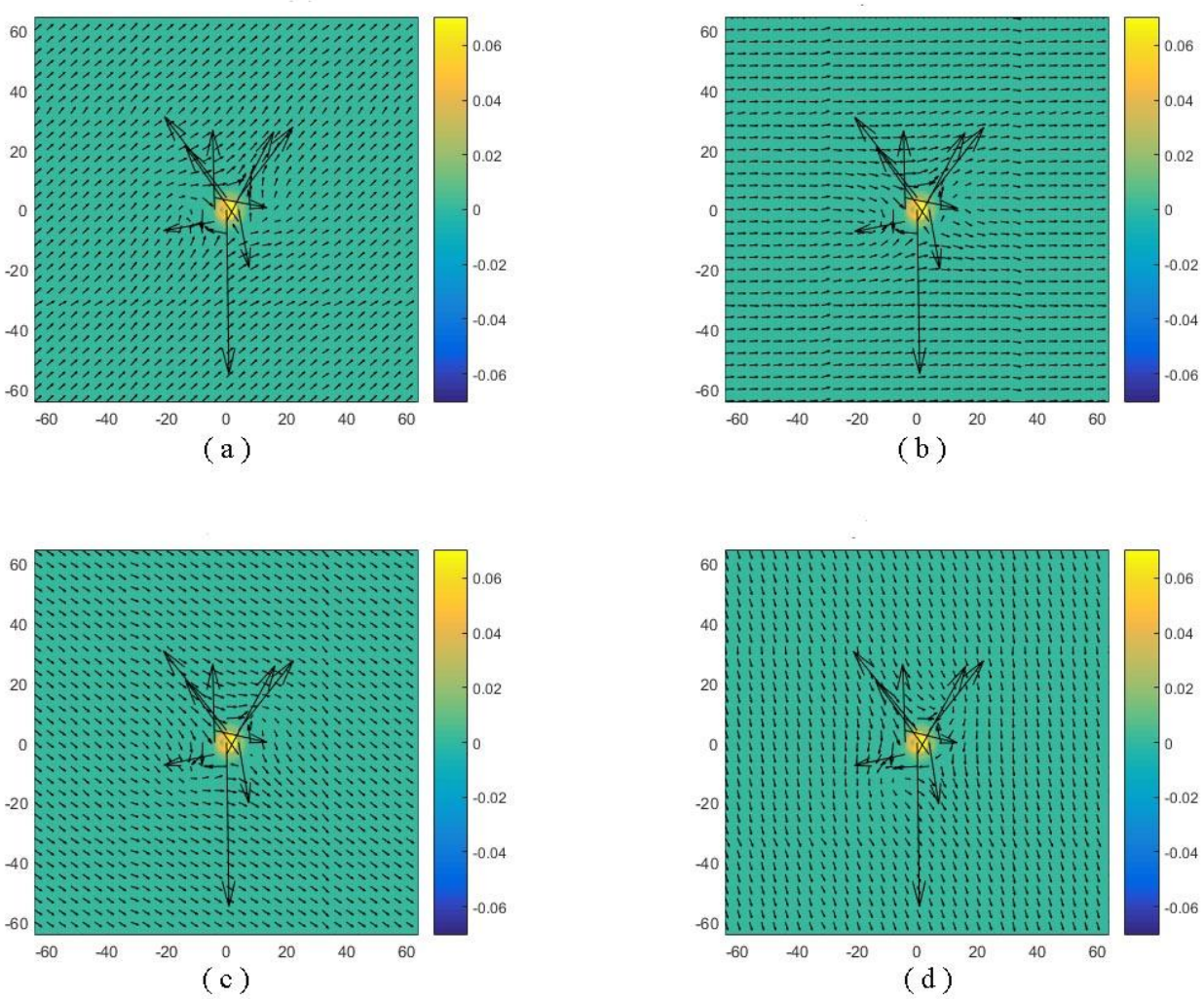

Fig 7: The spatial distributions of the vector of the bulk flow velocity of positive ions, $\boldsymbol{u_i}$, calculated for the second situation, correspondent to presence of the high-power high-frequency radio wave, in the plane perpendicular to the magnetic field. The normalized distances, $\boldsymbol{X}/\lambda_{De}^{0}$ and $\boldsymbol{Y}/\lambda_{De}^{0}$, that is, the distances in units of the Debye length, λ_{De}^{0}, from the central point of the simulation region are shown on the horizontal (***X***) and vertical (***Y***) axes. The vector of the magnetic field lies on the axis, perpendicular to the simulation region, and is directed downwards. The colouration of the figures indicates the module of the velocity in km/s. The results are given for the following moments: (a) $t = 98.6 \cdot T_{pe}$, (b) $t = 99 \cdot T_{pe}$, (c) $t = 99.4 \cdot T_{pe}$, (d) $t = 99.8 \cdot T_{pe}$.

It may be recalled that, at the initial moment, the bulk flow velocities of electrons and positive ions, $\boldsymbol{u_e}$ and $\boldsymbol{u_i}$ respectively, are assumed to be zero. It turns out that, for the first situation, correspondent to absence of an external electric field, the bulk flow velocities of electrons and positive ions, $\boldsymbol{u_e}$ and $\boldsymbol{u_i}$ respectively, were retained close to zero. For the second situation, correspondent to presence of the high-power high-frequency radio wave, the bulk flow velocities of electrons and positive ions, $\boldsymbol{u_e}$ and $\boldsymbol{u_i}$ respectively, rotate in each point of the two-dimensional simulation region, with modules of vectors of these flow velocities having essential values. These facts can be seen from Figures 6 and 7. It should be emphasized that modules of vectors of flow velocities of electrons are much more than absolute values of vectors of flow velocities of positive ions (Figures 6 and 7).

The normalized potential energy of the plasma, filling up all simulation region, is one of the physically significant parameters of the plasma. The time variations of this parameter, calculated for two considered situations, are presented in Figures 8. In both considered situations, the normalized potential energy of the plasma, filling up all simulation region, fluctuates, with the periods of the fluctuations being very similar. The fluctuations possess of two main periods, namely, the period of Langmuir oscillation of electrons and period of cyclotron oscillations of electrons. It is seen from Figure 8 that the time interval of about 50 equilibrium periods of Langmuir oscillations of electrons is sufficient for the normalized potential energy of the plasma, filling up all simulation region, to decrease and to achieve a stable regime for both considered situations.

It can be noticed that, in the course of time, the initially created irregularity in the concentration of charged particles lost its initial structure, was diffused, and decayed little by little in both considered situations correspondent to absence

and to presence of the external high-power high-frequency radio wave (bottom panel of Figure 1).

IV. CONCLUSIONS

Results of numerical simulations were presented of the time evolution of the super-small-scale irregularity in the electron concentration, created initially in the F-region ionospheric plasma. The simulation results were obtained

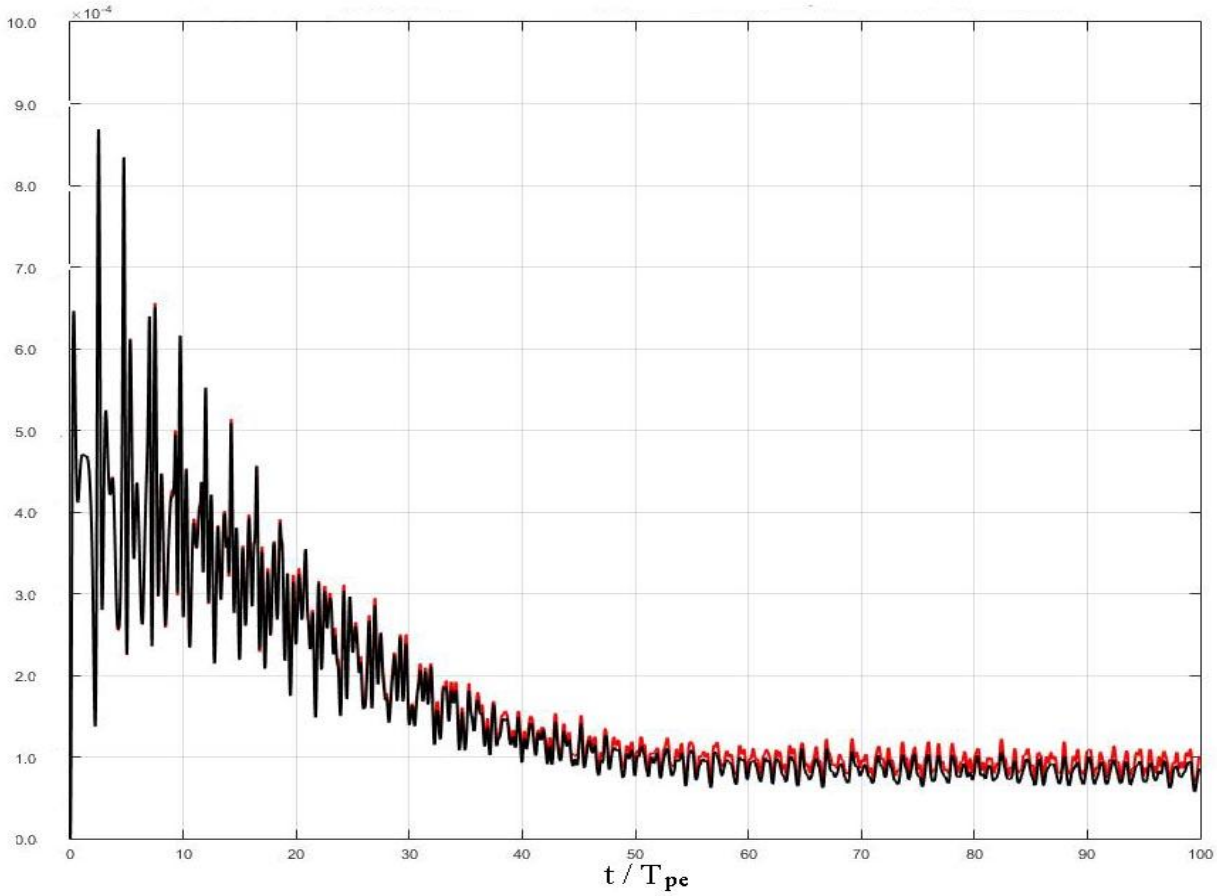

Fig 8: The time variation of the normalized potential energy of the plasma filling up all simulation region, $W_{pot}(t)/W_{kin}^{0}$ (in units of 10^{-4}). For the first situation, correspondent to absence of an external electric field, the results are shown by black line, whereas, for the second situation, correspondent to presence of the high-power high-frequency radio wave, the results are shown by red line. The normalized time, t/T_{pe}, that is, the time in units of the equilibrium period of Langmuir oscillations of electrons, T_{pe}, is shown on the abscissa.

by applying the two-dimensional mathematical model, developed earlier and based on numerical solving the Vlasov-Poisson system of equations by using the macroparticle method.

The investigated irregularity is supposed to be geomagnetic field-aligned, with its cross-section being circular. The initial cross-section diameter of the irregularity is equal to twelve Debye lengths of the plasma. In the applied version of the mathematical model, a motion of the positive ions is taken into account. Calculations were made using the input parameters of the model typical for the nocturnal F2-layer ionospheric plasma at the altitude of 300 km.

The simulation results were obtained for two distinct on principle situations. The first situation corresponds to absence of an external electric field, whereas the second situation corresponds to presence of the high-power high-frequency radio wave, pumped into the ionosphere by a ground-based ionospheric heater.

The results of simulation, obtained for two considered situations, have some common features. At the initial stage of time evolution, the initially created irregularities in the concentration of charged particles vanish and recover periodically in both considered situations, with the parameters of these irregularities fluctuating. In the course of time, the initially created irregularities in the concentration of charged particles lost their initial structures, were diffused, and decayed little by little.

However, the time variations of physical parameters at various points of the simulation region, in particular inside the irregularity, may be rather different for two considered situations. It turns out that a presence of external electric field which represents a high-power high-frequency radio wave, pumped into the ionosphere by a ground-based ionospheric heater, ought to influence significantly on the bulk flow velocities of electrons and positive ions. The vectors of these bulk flow velocities rotate in each point of the two-dimensional simulation region, with absolute values of vectors of flow velocities of electrons being much more than modules of vectors of flow velocities of positive ions. The rotations of the vectors of the bulk flow velocities of electrons and positive ions are conditioned by the action

of the rotating vector of the high-frequency wave's electric field.

ACKNOWLEDGMENT

The authors would like to thank the Editor and the anonymous referees for their careful reading and benevolent evaluation.

REFERENCES

[1] Moffet, R. J. and Quegan, S. (1983) The mid-latitude through in the electron concentration of the ionospheric F-layer: a review of observations and modelling. Journal of Atmospheric and Terrestrial Physics, 45, 315-343.
[2] Buchau, J., Reinisch, B. W., Weber, E. T., and Moore, J. G. (1983) Structure and dynamics of the winter polar cap F region. Radio Science, 18, 995-1010.
[3] Robinson, R. W., Tsunoda, R. T., Vickrey, J. F., and Guerin, L. (1985) Sources of F region ionization enhancement in the nighttime auroral zone. Journal of Geophysical Research, 90, 7533-7546.
[4] Ivanov-Kholodny, G.S., Goncharova, E.E., Shashun'kina, V.M., and Yudovich, L.A. (1987) Daily variations in the zonal structure of the ionospheric *F* region at low latitudes in February 1980. Geomagnetism and Aeronomia, 27(5), 722-727 (Russian issue).
[5] Tsunoda, R. T. (1988) High-latitude F region irregularities: A review and synthesis. Review of Geophysics, 26, 719-760.
[6] Besprozvannaya, A.S., Zherebtsov, G.A., Pirog, O.M., and Shchuka, T.I. (1988) Dynamics of electron density in the auroral zone during the magnetospheric substorm on December 22, 1982. Geomagnetism and Aeronomia, 28 (1), 66-70 (Russian issue).
[7] Muldrew, D. B. and Vickrey, J. F. (1982) High-latitude F region irregularities observed simultaneously with ISIS1 and Chatanika radar. Journal of Geophysical Research, 87 (A10), 8263-8272.
[8] Basu, S., Mac Kenzie, E., Basu, S., Fougere, P. F., Maynard, N. C., Coley, W. R., Hanson, W. B., Winningham, J. D., Sugiura, M., and Hoegy, W. R. (1988) Simultaneous density and electric field fluctuation spectra associated with velocity shears in the auroral oval. Journal of Geophysical Research, 93 (A1), 115-136.
[9] Martin, E. and Aarons, J. (1977) F layer scintillations and the aurora. Journal of Geophysical Research, 82, 2717-2722.
[10] Fremouw, E. J., Rino C. L., Livingston R. C., and Cousins M. C. (1977) A persistent subauroral scintillations enhancement observed in Alaska. Geophysical Research Letters, 4, 539-542.
[11] Kersley, L., Russell, C. D., and Pryse S. E. (1989) Scintillation and EISCAT investigations of gradient-drift irregularities in the high latitude ionosphere. Journal of Atmospheric and Terrestrial Physics, 51, 241-247.
[12] Pryse, S. E., Kersley, L., and Russell, C. D. (1991) Scintillation near the F layer trough over northern Europe. Radio Science, 26, 1105-1114.
[13] Greenwald, R.A. (1974) Diffuse radar aurora and the gradient drift instability. Journal of Geophysical Research, 79, 4807-4810.
[14] Dimant, Ya. S., Oppenheim, M. M., and Milikh, G. M. (2009) Meteor plasma trails: effects of external electric field. Annales Geophysicae, 27, 279-296.
[15] Wong, A. Y., Santoru, J., Darrow, C., Wang, L., and Roederer, J.G. (1983) Ionospheric cavitons and related nonlinear phenomena. Radio Science, 18, 815-830.
[16] Meltz, G. and LeLevier, R.E. (1970) Heating the F-region by deviative absorption of radio waves. Journal of Geophysical Research, 75, 6406-6416.
[17] Perkins, F.W. and Roble, R.G. (1978) Ionospheric heating by radio waves: Predictions for Arecibo and the satellite power station. Journal of Geophysical Research, 83 (A4), 1611-1624.
[18] Mantas, G.P., Carlson, H.C., and La Hoz, C.H. (1981) Thermal response of F-region ionosphere in artificial modification experiments by HF radio waves. Journal of Geophysical Research, 86 (A2), 561-574.
[19] Bernhardt, P.A. and Duncan, L.M. (1982) The feedback-diffraction theory of ionospheric heating. Journal of Atmospheric and Terrestrial Physics, 44, 1061-1074.
[20] Hansen, J.D., Morales, G.J., and Maggs, J.E. (1989) Daytime saturation of thermal cavitons. Journal of Geophysical Research, 94 (A6), 6833-6840.
[21] Vas'kov, V.V., Dimant, Ya.S., and Ryabova, N.A. (1993) Magnetospheric plasma thermal perturbations induced by resonant heating of the ionospheric F-region by high-power radio wave. Advances in Space Research, 13 (10), 25-33.
[22] Mingaleva, G.I. and Mingalev, V.S. (1997) Response of the convecting high-latitude F layer to a powerful HF wave, Annales Geophysicae, 15, 1291-1300.
[23] Mingaleva, G.I. and Mingalev, V.S. (2002) Modeling the modification of the nighttime high-latitude F region by powerful HF radio waves. Cosmic Research, 40 (1), 55-61.
[24] Mingaleva, G.I. and Mingalev, V.S. (2003) Simulation of the modification of the nocturnal high-latitude F layer by powerful HF radio waves. Geomagnetism and Aeronomy, 43 (6), 816-825 (Russian issue).
[25] Mingaleva, G.I., Mingalev, V.S., and Mingalev, I.V. (2003) Simulation study of the high-latitude F-layer modification by powerful HF waves with different frequencies for autumn conditions. Annales Geophysicae, 21, 1827-1838.
[26] Mingaleva, G.I., Mingalev, V.S., and Mingalev, I.V. (2009) Model simulation of the large-scale high-latitude F-layer modification by powerful HF waves with different modulation. Journal of Atmospheric and Solar-Terrestrial Physics, 71, 559-568.
[27] Mingaleva, G.I., Mingalev, V.S., and Mingalev, O.V. (2012) Simulation study of the large-scale modification of the mid-latitude F-layer by HF radio waves with different powers. Annales Geophysicae, 30, 1213–1222, doi:10.5194/angeo-30-1213-2012.
[28] Mingaleva, G.I. and Mingalev, V.S. (2013) Simulation study of the modification of the high-latitude ionosphere by powerful high-frequency radio waves. Journal of Computations and Modelling, 3(4), 287-309.
[29] Mingaleva G.I. and Mingalev V.S. (2014) Model simulation of artificial heating of the daytime high-latitude F-region ionosphere by powerful high-frequency radio waves // International Journal of Geosciences, Volume 2014(5), 363-374.
[30] Eliasson, B. and Stenflo, L. (2008) Full-scale simulation study of the initial stage of ionospheric turbulence. Journal of Geophysical Research, 113 (A2), A02305.
[31] Mingalev, O.V., Mingalev, I. V., and Mingalev, V. S. (2006) Two-dimensional numerical simulation of dynamics of small-scale irregularities in the near-Earth plasma. Cosmic Research, 44 (5), 398-408.
[32] Mingalev, O.V., Mingaleva, G. I., Melnik, M.N., and Mingalev, V. S. (2010) Numerical modeling of the behavior of super-small-scale irregularities in the ionospheric F2 layer. Geomagnetism and Aeronomy, 50(5), 643-654.
[33] Mingalev O.V., Melnik M.N., Mingalev V.S. Numerical modeling of the time evolution of super-small-scale irregularities in the near-Earth rarefied plasma // International Journal of Geosciences.-2015.-V. 6. P. 67-78.
[34] Hockney, R.W. and Eastwood, J.W. (1981) Computer simulation using particles. McGraw-Hill. New York.
[35] Birdsall, C.K. and Langdon, A.B. (1985) Plasma physics via computer simulation. McGraw-Hill. New York.